Journal of Alloys and Compounds, 195 (1993) 23–26
JALCOM 7406

MELT PROCESSING OF POWDERED ARC-CAST $YBa_2Cu_3O_y$ MATERIALS

E.YANMAZ, A. DRAKE, I.R.HARRIS AND J.S. ABELL
School of Metallurgy and Materials Science, University of Birmingham, Birmingham B15 2TT, UK.

We report the Arc-Quench-Powder-Growth (AQPG) process as a modification of the QMG technique. Pellets of YBa_2Cu_3Oy were quenched by arc-casting in a water cooled mould and then crushed to give powder which was compacted and then subjected to a melt growth process. As a result of this processing, large grained textured YBCO material was produced. The microstructure and physical properties of these AQPG samples were investigated when subject to various temperature cycles. It was found that the volume fraction and size distribution of the second phase inclusions were dependent upon the maximum temperature during the melt growth process. Critical currents of the samples have been measured by magnetisation using a VSM.

1. Introduction

Various methods of melt processing have been reported[1-4] which have been designed to produce textured grain alignment and associated microstructural modifications, in order to enhance flux pinning and thus increase current-carrying capacities. Among these techniques, melt-textured growth (MTG) [1], quench melt growth (QMG) [2], melt powder melt growth (MPMG) [3] and zone melting [4] have been applied to the YBCO system.

In this paper, we have attempted to produce large grained, textured YBCO material from a precursor material of powdered arc-cast YBCO. This modified preparation process will be refered to as the Arc-Quench-Powder-Growth (AQPG) process. The microstructure and superconducting properties of AQPG samples have been examined and measured and will be described

2. Experimental Procedure

Appropriate amounts of Y_2O_3, $BaCO_3$ and CuO in the 123 ratio were well-mixed and calcined at 900°C for 8h in air. This calcined powder was then pressed into pellets after a grinding process. These pellets were melted in a non-consumable electrode arc furnace and cast into rods by sucking the liquid into a water cooled copper mould[5].

After solidification the YBCO (123) rods were crushed to powder and mixed using a mortar and pestel machine. The yellow powders were then pressed into pellets and reheated to 1100°C for 20 minutes in air, and then cooled to 1000°C at a rate of 100°C/h, followed by 1°C/h to 950°C. When the temperature dropped to 950°C, the sample was allowed to cool to room temperature by step cooling. All of this processing was carried out on a Pt sheet to reduce contamination.

Finally, the samples were annealed at 600°C for 1h in flowing oxygen and slow cooled. The schematic illustration of the arc-quench-powder-growth (AQPG) is shown in figure1.

The microstructures of the precursor material and AQPG material were studied by polarized light optical microscopy and scanning electron microscopy (SEM). The phases present were determined using energy dispersive X-ray (EDX) analysis and X-ray diffraction (XRD). The superconducting transition temperatures were determined by a.c. susceptibility and resistivity measurements.

The critical current density (Jc) was estimated from magnetization loops which were determined by a vibrating sample magnetometer (VSM) using a magnetic field up to 4 tesla with a sweep rate of 5mT/sec. The field was applied perpendicular to the c-axis of the aligned grains. From the microscopic studies the average grain size was taken to be 0.27x0.7x0.16 cm^3.

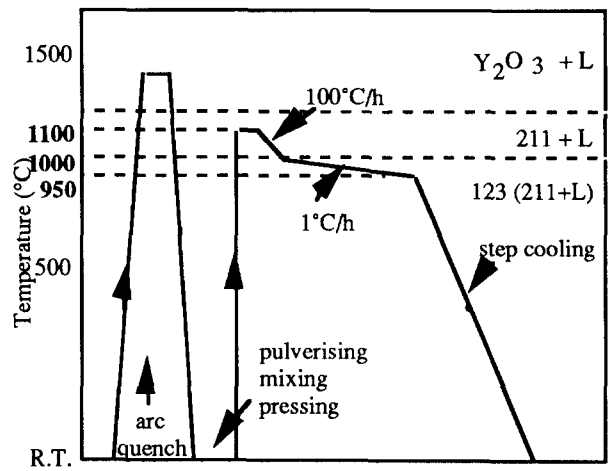

Figure 1. Schematic illustration of AQPG process.

3. Results and Discussion

The phase relation with temperature for melt processed Y-Ba-Cu-O system has been investigated by many groups [4, 6-8] and reported the following two reactions in the Y-Ba-Cu-O system:

$$2YBa_2Cu_3O_7 \rightarrow Y_2BaCuO_5 + L\ (3BaCuO_2+2CuO) \quad (1)$$
$$Y_2BaCuO_5 \rightarrow Y_2O_3 + L\ (BaO + CuO) \quad (2)$$

where L denotes the liquid phase. As the temperature is increased, the 123 phase first decomposes into the 211 phase and liquid (e.q 1) and then further decomposes into Y_2O_3 and the liquid (eq.2) at temperatures in exess of 1200°C [9]. It has been reported [6,7,9,10] that when the distribution of Y_2O_3 is uniform, the final distribution of

0925-8388/93/$06.00

211 in the solid becomes homogenous, and to avoid the reaction and coarsening of Y_2O_3, the YBCO material should be heated rapidly to the Y_2O_3 + L region and quenched soon after the sample has melted [3].

The SEM micrographs taken from the cross-section of a cast rod are shown in Figure 2. Three different phases were determined by EDX analysis to be Y_2O_3 (I in Figure 2a), liquid phase (II in Figure 2a) and Y_2BaCuO_5 (III in Figure 2b).

It can be seen clearly that the Y_2O_3 particles are distributed in the liquid phase, but when the whole cross-section of the rod was examined it was found that the distribution was not homogenous. However, the micrographs shown in figure 2 demonstrate that it is easy to enter the Y_2O_3 + L phase field using an arc-casting method. The presence of 211 phase (III in Figure 2b) in the central region of the rod indicates that the solidification rate may not be sufficient in the central region to suppress the formation of 211 phase.

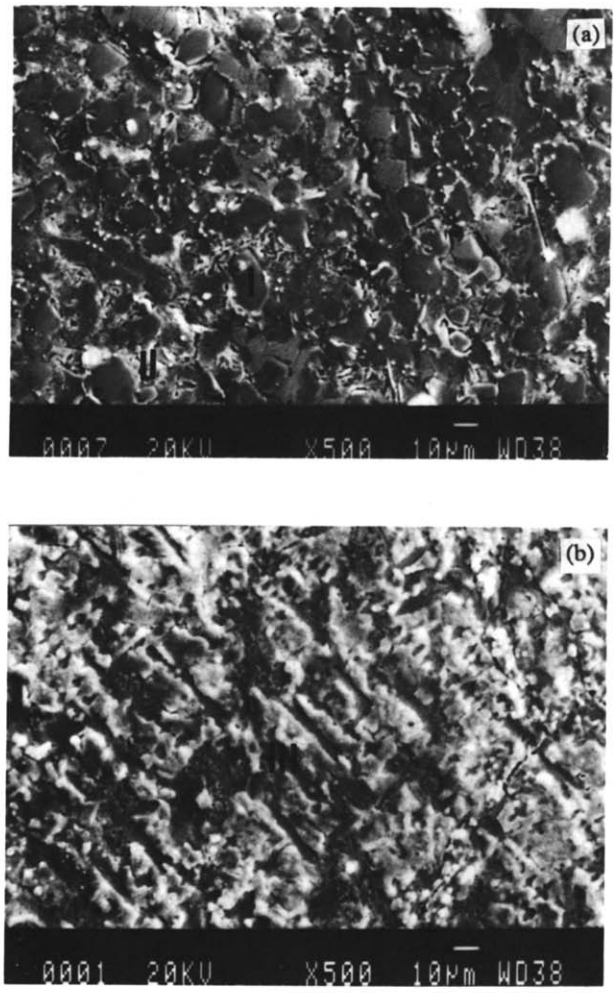

Figure 2. SEM micrographs of arc-cast 123 material indicate (a) distribution of Y_2O_3 particles in the liquid phase and (b) the 211 phase in the long needle form.

In order to obtain a homogenous distribution of particles in the liquid phase, prior to melt processing, the arc-cast rods were crushed into a powder and mixed before pressing into pellets. The melt processing treatment shown in figure1 was then applied to these pellets.

During this treatment the pellets are re-heated into the 211 + L region (1100°C). At this temperature the Y_2O_3 particles react with the liquid phase and result in the nucleation of 211 phase in accordance with the phase diagram [2].

Following the heat treatment at 1100°C, the samples were cooled to 1000°C at the rate of 100°C/h. During cooling, the 211 phase reacts with the liquid phase (mixture of $BaCuO_2$ and CuO) and forms the 123 phase. Further cooling to 950°C at the rate of 1°C/h allows the 123 grains to grow [2-4].

Figure 3 shows optical micrographs of an as-grown AQPG sample. The micrographs indicate large grained and textured 123 crystals with inclusions of 211 precipitates. It can be seen in figure 3a that the precipitates

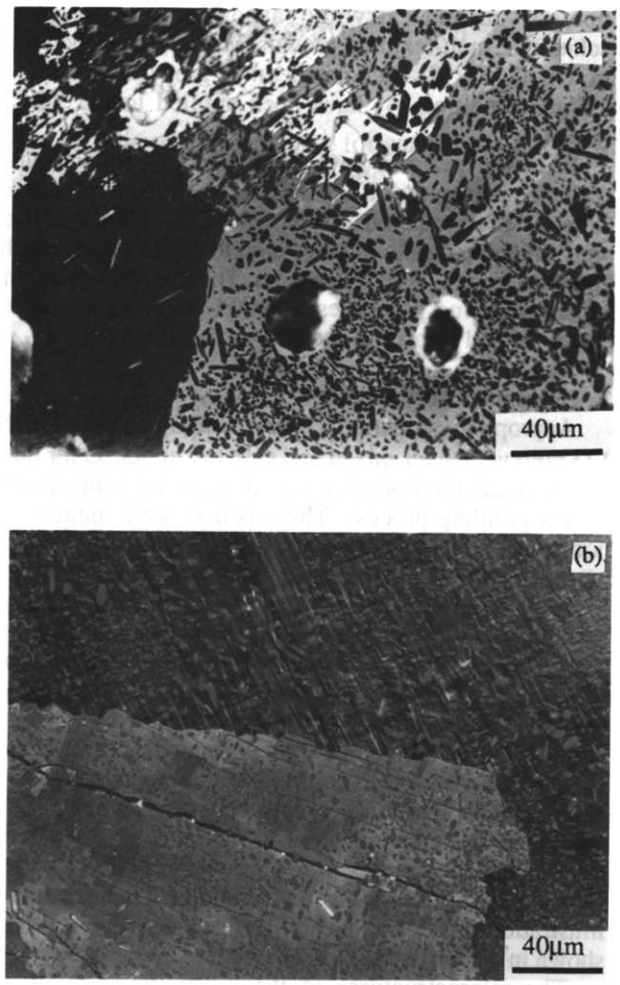

Figure 3. (a) Optical micrographs of an as-grown sample of AQPG indicate large grain of 123 phase with inclusion of 211 precipitates. Additionally, some cracks shown in (b), which are almost parallel to each other, and occur within a grain perpendicular to the c-axis direction.

are both ellipsoidal and spherical in shape and are dispersed with a spacing of several micrometers. The micrographs have grains with different contrast due to the different crystal orientations revealed using polarized light.

The boundaries between large 123 grains were generally found to be clean and contained no impurity phases giving good connectivity between the grains. It can also be seen (figure 3b) that some cracks, which are nearly parallel to each other, form within the grains perpendicularly to the c-axis direction. It is thought that this is caused by the tetragonal to orthorhombic phase transformation and oxygen absoption which occur during cooling[3, 7].

The microstructures of these samples have also been examined at higher magnifications in a transmission electron microscope. A TEM micrograph of a sample after oxygenation is shown in figure 4. This shows the twins which are characteristic of oxygenated YBCO together with dislocations and a high density of stacking faults. This density of defects is much greater than that observed in flux grown single crystals where 123 forms as the primary phase from a liquid but is typical of these melt processed materials where 123 forms from a peritectic reaction. It is thought that it is these types of defects which increase the critical current in melt processed materials.

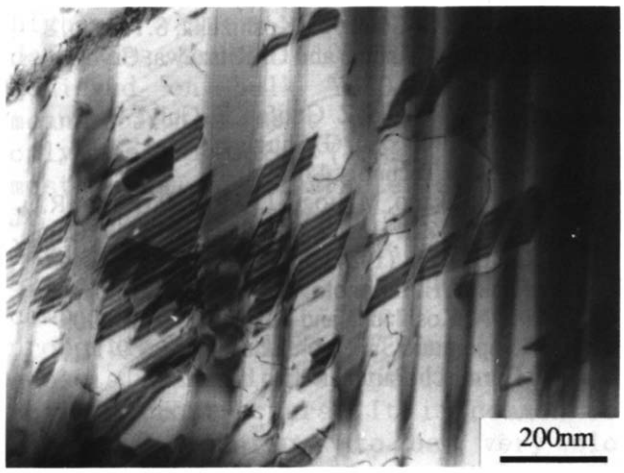

Figure 4. A TEM micrograph of a sample after oxygenation.

The temperature dependence of normalised a.c. susceptibility and resistivity for as-grown and annealed specimens are shown in figure 5 and figure 6 respectively. As can be seen in both figures, the superconducting transition became sharper after annealing the as-grown specimen at 600°C for 1 hour in flowing oxygen. The onset transition temperature for both samples are almost the same (figure 5) which are round 92K, but, the zero resistance transition temperatures (figure 6) for as-grown and annealed specimens were found to be 85K and 91K respectively. This result suggests that the as-grown sample is insufficiently oxygenated and must be oxygen annealed to optimise the transition temperature.

Figure 7 shows magnetisation hysteresis loops of 1h annealed specimen measured at 4.2K, 50K and 77K under a 4 tesla magnetic field using a vibrating sample magnetometer (VSM). The difference in magnetization increases with decreasing temperature. At 77K, the magnetization value almost became zero in a magnetic field of 4 tesla. This indicates that the magnetic field easily penetrates into the superconducting grains at 77K at these fields.

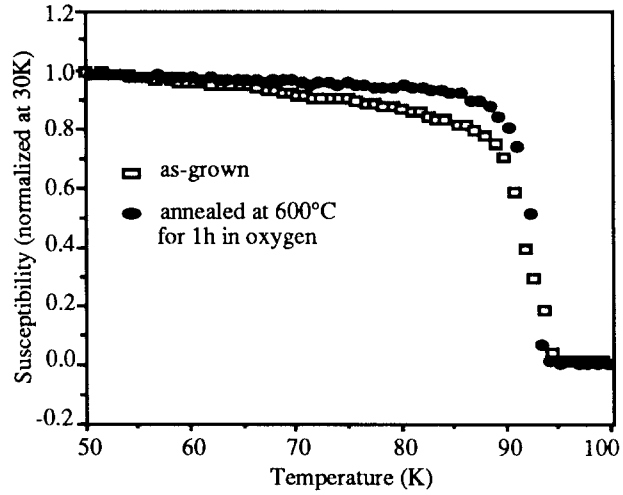

Figure 5. Normalised ac. susceptibility of an as-grown sample and a 1h annealed in flowing oxygen sample.

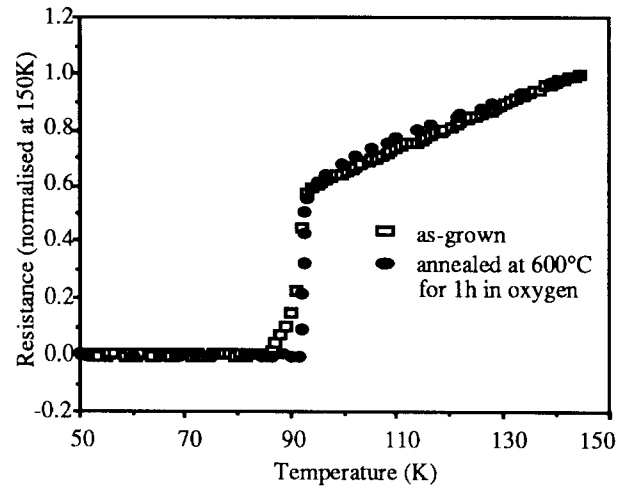

Figure 6. Normalised resistivity curves of samples before and after annealing at 600°C for 1h in oxygen.

Figure 8 shows the magnetic field dependence of critical current density, J_C. The estimation of J_C from the magnetization hysteresis loops were performed using Bean's Critical State Model[2,3,6,7,10]. The relation is indicated by the following equation:

$$4\pi (M^+ - M^-) = (4\pi/10)\, J_C\, (d/2) \qquad (3)$$

where M^+ and M^- are magnetization in the increasing and decreasing field process in emu/cm^3, J_C is the critical

current density in A/cm^2 and d is the sample thickness in cm. The field dependences of Jc at different temperatures show different behaviour. As can be seen, the variation of J_c changes almost linearly with increasing field at 4.2K while it is changing exponentially at 50K and 77K upto 1 tesla and then a gradual decrease. The Jc values in zero field at 4.2K, 50K and 77K were estimated to be 1.2 x10^5 A/cm^2, 2x10^4 A/cm^2 and 5x10^3 A/cm^2, respectively and these values decrease with increasing magnetic field.

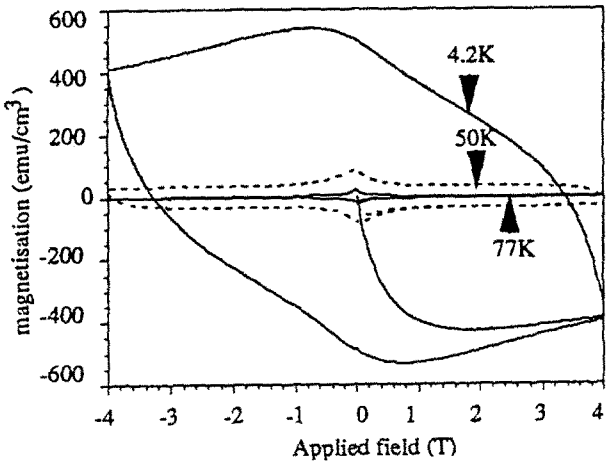

Figure 7. Magnetization hysteresis loops at 4.2K, 50K and 77K under 4 tesla magnetic field for 1h annealed of an as-grown specimen.

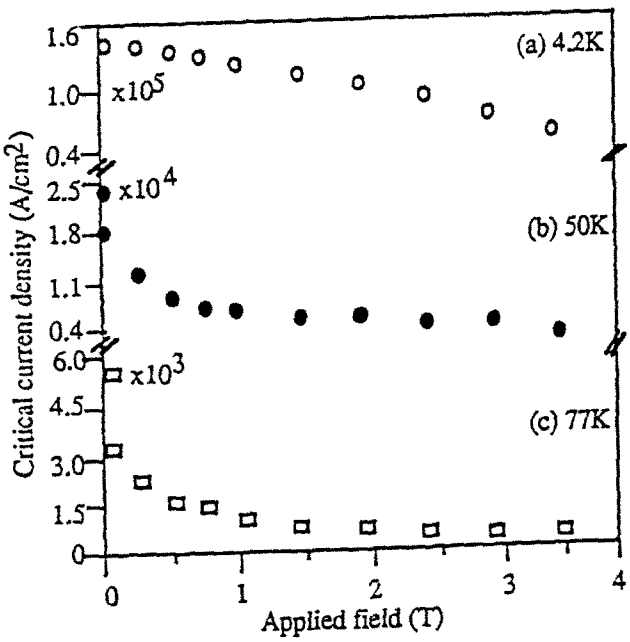

Figure 8. Magnetic field dependence of critical current densities at various temperatures for 1h annealed specimen.

4. Conclusion.

Arc casting is a possible route by which a fine dispersion of the 211 phase in YBCO can be achieved, and if the melt annealing temperatures and times are optimised it should be possible to produce high Jc material from this precursor.

Acknowledgements

Thanks are due to the SERC and to the EC (twinning Programme) for their support of the research programme in high-T_c superconductors. Thanks are also due to the Karadeniz Technical University, Trabzon, Turkey, for the provision of a studentship (EY).

References

1 S.Jin, T.H.Tiefel, R.C.Sherwood, R.B.van Dover, M.E.Davis, G.W.Kommlott, and R.A.Fastnacht, Phys.Rev.B37 (1988) 7850.
2 M.Murakami, Modern Phys.Lett.B 4(3) (1990) 163.
3 M Murakami, T Oyama, H Fujimoto, S Gotoh, K Yamaguchi, Y Shiohara, N Koshizuaka and S Tanaka, IEEE Transactions on Magnetics 27(2) (1991) 1479.
4 J Kase, J Shimoyama, E, Yanagisawa, S Kondoh, T Matsubara, T Morimoto and M Suzuki, Jpn.J.Appl.Phys.29(2) (1990) L277.
5 E.Yanmaz, J.S.Abell and I.R.Harris, J.Less-comm.Metals 164 & 165 (1990) 193.
6 M. Murakami, Supercurrents, July (1989) 41
7 M. Murakami, S. Gotoh, N. Koshizuka, S.Tanaka, T.Matsushita, S. Kambe and G. Kitazawa, Cryogenics 30 (1990) 390.
8 J. Chulin, F. Zhanguo, Z. Guofan, Z. Guiyi, B. Weimin, Z. Zhongxian, G. Shuguan Supercond.Sci.Technol..,4 (1991) 49.
9 K. Oka, K. Nakano, M. Ito, C.J. Torng, P.H. Hor, R.L. Meug, L. Gao, Z.J. Huang, Q. Wang, and C.W. Chu, Phys.Rev.Lett., 58 (1987) 908.
10 M. Murakami, H. Fujimoto, T. Oyama, S. Gotoh, Y. Shiohara, N. Koshizuka and S. Tanaka, ICMC'90 High-Temperature Superconductivity, May 9-11, (1990) Garmisch-Partenkirchen, Germany.